This is the Pre-Published Version.

The following publication Z. Dong, M. Jiang, S. Niu and K. T. Chau, "Mechanical Flux-Weakening Design of the Bidirectional Flux-Modulated Radial Permanent Magnet Generator for Wind Power Generation," in IEEE Transactions on Magnetics, vol. 61, no. 9, pp. 1-5, Sept. 2025, Art no. 8101605 is available at https://doi.org/10.1109/TMAG.2025.3531139.

Mechanical Flux-Weakening Design of the Bidirectional Flux-Modulated Radial Permanent Magnet Generator for Wind Power Generation

Zixu Dong, Mingyuan Jiang, Shuangxia Niu, and K. T. Chau, *Fellow, IEEE*

Department of Electrical and Electronic Engineering, The Hong Kong Polytechnic University, Hong Kong

Wind power plays an important role in the transition to new energy sources. This article introduces a bidirectional flux-modulated radial permanent magnet (PM) generator, incorporating a mechanical flux-weakening design. The focus is on achieving mechanical flux-weakening effects through the principles of flux modulation while employing working harmonics to ascertain the appropriate winding pole pair number and sequence. This design facilitates the regulation of the induced back electromotive force (EMF) and enables a broad operational speed range for the variable speed constant amplitude voltage (VSCAV) mode of the wind power generator. Furthermore, the strategic selection of specific working harmonics permits the generator to operate with a singular set of windings. The topology is presented, and the operational principles are thoroughly analyzed. Ultimately, the structure is subjected to testing through algorithm optimization and finite element method (FEM).

***Index Terms*— Finite element method (FEM), flux modulation principle, mechanical flux weakening, permanent magnet (PM) machine, radial type, wind power generation, working harmonics.**

I. Introduction

With the escalation of climate change and the diminishing availability of fossil fuel resources, there is an increasing awareness of the unsustainability of depending on conventional energy sources. Therefore, the imperative to shift toward renewable energy has become more pressing than ever, wind power generation has emerged as a pivotal element in the global renewable energy landscape, necessitating advancements in generator design to enhance efficiency, reliability, and performance across diverse wind conditions [1], [2]. Permanent magnet (PM) generators hold a significant position in the field of wind power generation due to their advantages of high efficiency, high power density, and enhanced reliability [3], [4], [5].

In wind power generation, wind speed is not constant and can vary over a wide range, making the control of output voltage a complex issue. Furthermore, the fixed magnetic flux of PMs influences the operating speed of the generator. Therefore, implementing flux-weakening control in PM wind power generators enables operation across a broad spectrum of wind speeds while maintaining effective control over the voltage.

The conventional method for flux-weakening is to inject a negative d-axis current, which generates a magnetic field that counteracts the magnetic field provided by the PMs, thereby reducing the magnetic flux [6], [7], [8]. However, if an excessive amount of negative d-axis current is injected, there is a risk of demagnetization of the PMs. In [9], [10], and [11], a winding switching strategy is proposed to achieve flux weakening, and however, this method involves complex control circuits and introduces additional losses. Moreover, for hybrid excited machines, excitation current can be supplied to additional excitation windings to control the magnetic flux, with the polarity of the excitation current being adjusted to enhance or reduce the magnetic flux [12], [13]. The excitation path is typically arranged in parallel with the magnetic circuit of the PMs to prevent demagnetization of the PMs. In addition, magnetic flux can be controlled using a memory machine [14], [15], which involves injecting current pulses into the PM machine to alter the magnetization state of low coercivity PMs, thereby adjusting the magnetic flux in the air gap. Depending on the configuration of the current pulse injection coils, memory machines can be categorized into self-coiling and super-coiling types. However, the structure of memory machines tends to be relatively complex.

However, regardless of the aforementioned specific electrical method employed, additional energy consumption is required, usually in 5%–20% power loss, which adversely affects the overall efficiency of the system. Mechanical flux weakening can be realized without the need for extra energy consumption, as it involves adjusting the angle of a particular component within the machine. This approach also mitigates the risk of PM demagnetization. Zhu et al. [16] proposed switched flux PM machines with flux adjusters located on the outside surface of the stator, which achieves the effect of flux weakening. In [17], the rotor is segmented into two parts by utilizing auxiliary mechanisms such as brakes, and the magnetic flux is regulated through the relative motion between the two rotors and the stator. Jiang and Niu [18] presented a PM generator for wind power generation with mechanical flux weakening based on flux modulation principles.

The principle of flux modulation is widely applied in PM machines [19], [20], [21], [22]. By regulating the magnetic flux, it enhances the efficiency and performance of the machine while broadening the speed control range. Jiang et al. [20] proposed a dual-rotor transverse flux PM machine, and two rotors operated at a lower counter-rotational speed generate a high-frequency magnetic flux density in the air gap based on the principle of flux modulation, thereby enhancing the system's rotational speed. The generator proposed in [21]

© 2025 IEEE. Personal use of this material is permitted. Permission from IEEE must be obtained for all other uses, in any current or future media, including reprinting/republishing this material for advertising or promotional purposes, creating new collective works, for resale or redistribution to servers or lists, or reuse of any copyrighted component of this work in other works.

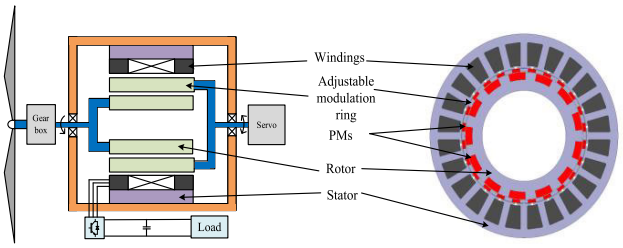

Fig. 1. Configuration of the generator topology and generating system.

and [22], which is based on the principle of bidirectional flux modulation, can significantly improve the performance of the generator and is suitable for direct-drive applications.

Currently, mainstream generators rarely employ the mechanical flux-weakening method, which not only consumes additional energy but also decreases the system's reliability. Furthermore, most generators utilize two sets of windings, increasing costs and complicating the manufacturing process. To deepen the understanding of mechanical flux weakening and the principle of flux modulation, this study introduces a bidirectional flux-modulated radial PM generator (BFRPMG) featuring a mechanical flux-weakening design. The mechanical topology and working principles are explained. In addition, the generator's performance is enhanced using an optimization algorithm aimed at increasing torque density and minimizing torque fluctuations. The analysis of the structure is conducted using finite element method (FEM) simulations. The rest of this article is arranged as follows. Section II proposes the machine configuration with machine topology. Section III introduces working principles, including bidirectional flux modulation principle and working harmonic selection. In Section IV, the optimization of the structure and the performance after optimization are analyzed. Finally, conclusions are summarized in Section V.

II. Machine Configuration

The mechanical topology of the PM generator is illustrated in Fig. 1, which provides a detailed representation of the components within the power generation system and their interrelations. From Fig. 1, it can be observed that the generator is equipped with two mechanical ports (MPs). The first MP, i.e., the rotor, is linked to the wind turbine blades via a gearbox, thus effectively converting wind energy into mechanical power. The second MP is the adjustable modulation ring, which can alter its angular position under the control of a servo motor, thereby enabling precise modulation of the magnetic flux in the air gap.

The design incorporates 13 pole pairs of PMs that are inserted into the rotor and oriented in a radial direction. This innovative approach allows for efficient modulation of the magnetic field in the air gap. Moreover, each adjustable modulation ring is equipped with PMs that align with the magnetization direction of the PMs in the rotor, facilitating a bidirectional magnetic flux effect. Meanwhile, both the rotor and the adjustable modulation ring form the consequence-pole structure. The number of pole pairs on the adjustable modulation ring is 24, which corresponds to the number of stator slots, ensuring a harmonious interaction between the modulation capabilities of generator and the output from stator.

A three-phase winding arrangement of 13 pole pairs is deployed in the stator slots, utilizing a single-layer winding

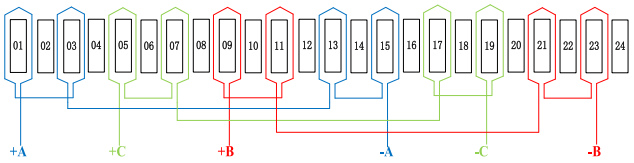

Fig. 2. Diagram of the winding configuration distribution.

configuration. This design simplifies the manufacturing process and significantly reduces production costs. Fig. 2 further elucidates the distribution of the winding according to the slot potential vector.

III. Working Principles

A. Bidirectional Flux Modulation Effect

In recent years, the bidirectional flux modulation effect based on flux modulation effect has been widely researched. Fig. 3 illustrates a part of the machine, serving to explain the phenomenon of bidirectional flux modulation effect. As shown in Fig. 3, the rotor PMs and the adjustable modulation rings form the first flux modulation group, while the rotor teeth and the PMs between adjustable modulation rings form the second flux modulation group. In the following, the first flux modulation group is selected as an example to illustrate the bidirectional flux modulation effect.

The fundamental component of magnetic motive force (MMF) of the rotor PMs $F_r(\theta,\theta_1)$ and the magnetic circuit permeance of the air gap 1 $P_{\text{gap1}}(\theta)$ can be expressed as follows:

$$\begin{aligned} F_r(\theta,\theta_1) &= F_1\cos[N_r(\theta-\theta_1)] \\ &= \frac{\pi}{4}\frac{h_m}{\mu_m}B_r\cos[N_r(\theta-\theta_1)] \end{aligned} \tag{1}$$

$$P_{\text{gap1}}(\theta) = P_0 - P_1\cos[N_m(\theta-\theta_2)] \tag{2}$$

where N_r is the pole pair number of rotor and N_m is the pole pair number of adjustable modulation ring. θ, θ_1, and θ_2 are the angular position of the air-gap field, the rotor, and the adjustable modulation ring, respectively, as shown in Fig. 3. F_1 is the amplitude of MMF at θ_1, and P_0 and P_1 are parameters depending on the slot dimensions and empirical coefficients. h_m, μ_m, and B_r are all properties of PMs, respectively, the thickness, the relative magnetic permeability, and the remanence.

Therefore, the flux density in the air gap can be obtained by multiplying $F_r(\theta,\theta_1)$ and $P_{\text{gap1}}(\theta)$, which can be calculated as follows:

$$\begin{aligned} &B_{\text{gap1}}(\theta,\theta_1) \\ &= F_r(\theta,\theta_1)P_{\text{gap1}}(\theta) \\ &= \frac{\pi}{4}\frac{h_m}{\mu_m}B_r\left\{\begin{array}{l} P_0\cos[N_r(\theta-\theta_1)] \\ -\frac{P_1}{2}\cos[(N_r-N_m)\theta-(N_r\theta_1-N_m\theta_2)] \\ -\frac{P_1}{2}\cos[(N_r+N_m)\theta-(N_r\theta_1+N_m\theta_2)] \end{array}\right\}. \end{aligned} \tag{3}$$

The flux linkage can be obtained by integrating the flux density, which is expressed as follows:

$$\psi(\theta_1) = Nr_g l_{eg}\int_0^{\frac{\pi}{N_Z}} B_{\text{gap1}}(\theta,\theta_1)d\theta \tag{4}$$

where r_g is the air-gap radius, l_{eg} is the axial length, N is the number of turns of coil, and N_Z is the pole pair number of winding. According to (3) and (4), the flux density due to the flux modulation effect with $N_r \pm N_m$ is negligible if $N_r = N_m$. For $N_r \neq N_m$, P_0 is much smaller than P_1 due to the adjustable modulation rings and the flux linkage can be expressed as follows:

$$\begin{aligned}\psi(\theta_1) &= N r_g l_{eg} \int_0^{\frac{\pi}{N_Z}} B_{\text{gap1}}(\theta, \theta_1) d\theta \\ &= N r_g l_{eg} \frac{\pi}{4} \frac{h_m}{\mu_m} B_r \\ &\quad \times \left[\frac{k_{w0} P_0}{N_r} \sin(N_r \theta_1 + \varphi_0) \right. \\ &\quad + \frac{k_{w1} P_1}{N_Z} \sin(N_r \theta_1 - N_m \theta_2 + \varphi_1) \\ &\quad \left. + \frac{k_{w2} P_1}{N_r + N_m} \sin(N_r \theta_1 + N_m \theta_2 + \varphi_2) \right] \end{aligned} \quad (5)$$

where k_{w0}, k_{w1}, and k_{w2} are the winding factors of N_r, N_m, and $N_r + N_m$ harmonic field, respectively. φ_0, φ_1, and φ_2 are the phase shift. According to (5), $k_{w1} = 1$ and much higher than k_{w0} and k_{w2} when $N_Z = N_m - N_r$; therefore, (5) can be expressed as follows:

$$\psi(\theta_1) = N r_g l_{eg} \frac{\pi}{4} \frac{h_m}{\mu_m} B_r \frac{P_1}{N_Z} \sin(N_r \theta_1 - N_m \theta_2) \quad (6)$$

where $\theta_1 = \Omega_1 t$, with Ω_1 being the rotating speed of rotor. Moreover, the back electromotive force (EMF) can be derived from the derivative of the flux linkage, which is expressed as follows:

$$\begin{aligned} E(t) &= \frac{d\psi}{dt} \\ &= N r_g l_{eg} \frac{\pi}{4} \frac{h_m}{\mu_m} B_r \frac{P_1}{N_Z} \\ &\quad \times N_r \Omega_1 \cos(N_r \Omega_1 t - N_m \theta_2). \end{aligned} \quad (7)$$

The second group of flux modulation operates on a principle similar to that of the first group, generating back EMF that shares a common winding configuration with the first group. The specific theoretical framework will be elucidated in Section III-B discussing the selection of working harmonics.

B. Working Harmonics Selection

Based on the principle of flux modulation, (1) and (2) can be expressed in another way as follows:

$$F_r(\theta, t) = \sum_{j=1,3,5,\ldots} F_j \cos\left[j N_r (\theta + \Omega_1 t) \right] \quad (8)$$

$$P_{\text{gap1}}(\theta, \phi) = P_0 + \sum_{k=1,2,3,\ldots} P_k \cos[k N_m (\theta + \phi)]. \quad (9)$$

According to (8), the maximum of MMF can be achieved when $j = 1$. The highest value of magnetic circuit permeance of the air gap can be obtained when $k = 1$ according to (9). Therefore, the harmonics with $j = 1$ are utilized as working harmonics for Types 0, 1, and 2. The harmonics with $k = 1$ are working harmonics for adjustable modulator ring in Types 1 and 2, where Type 0 components are unmodulated stationary components, Types 1 and 2 are both modulated components, Types 0 and 1 rotate in the same direction, and Type 2 rotates in the opposite direction of Type 0. Consequently, it can be inferred that all working harmonics possess the same frequency, thereby facilitating the output of back EMF through a singular set of windings.

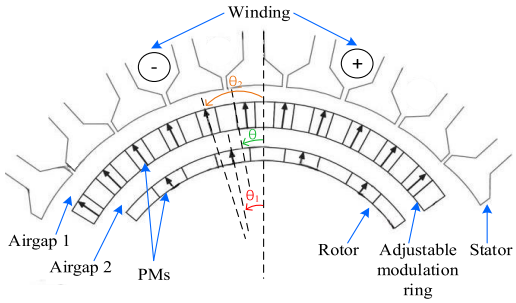

Fig. 3. Part of the structure diagram.

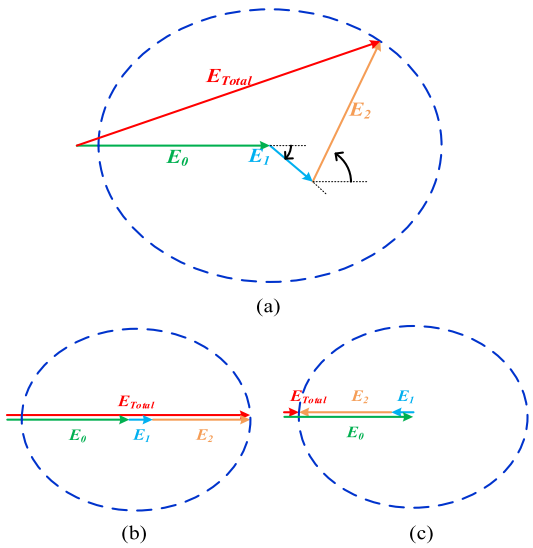

Fig. 4. Vector graph of back EMF. (a) Showing diagram. (b) Maximum total back EMF position. (c) Minimum total back EMF position.

Designing the number of adjustable modulation rings to correspond with the number of stator slots allows for the maximized utilization of working harmonics [18]. All harmonics possess the same order and can be directly vectorially summed. Fig. 4 shows the back EMF vector graph. It can be found that the total back EMF reaches its maximum when the electrical initial phase angle of the modulator is $\Omega = 0°$, while the minimum is achieved at $\Omega = 180°$. This allows for a wide range of adjustment for the total back EMF, spanning from $|E_0 - E_1 - E_2|$ to $(E_0 + E_1 + E_2)$.

IV. Optimization and Analysis of Machine

The preliminary design of the structure in this article will undergo optimization through the nondominated sorted genetic algorithm-II (NSGA-II) to maximize torque density and minimize torque fluctuations. Table I shows the parameters of the optimized structure.

Fig. 5 shows the back EMF curves of the design at no load. FEM simulations were conducted on the optimized structure, resulting in a back EMF amplitude of 1.45 V for a single-turn coil. The optimized structure features a stator slot area of 308.22 mm^2, allowing for the accommodation of

TABLE I

PARAMETERS OF OPTIMIZED GENERATOR

Items	Unit	Value
Angle of modulation ring	mech. deg	7.5°
Angle of PMs	mech. deg	11.08°
Width of stator teeth	mm	6.96
Height of rotor PMs	mm	6.86
Height of modulator	mm	3.01
Height of stator slot	mm	20.6
Height of stator yoke	mm	8.21
Height of rotor yoke	mm	10.1
Number of stator slot	N/A	24
Stator outer diameter	mm	190
Airgap length	mm	0.5

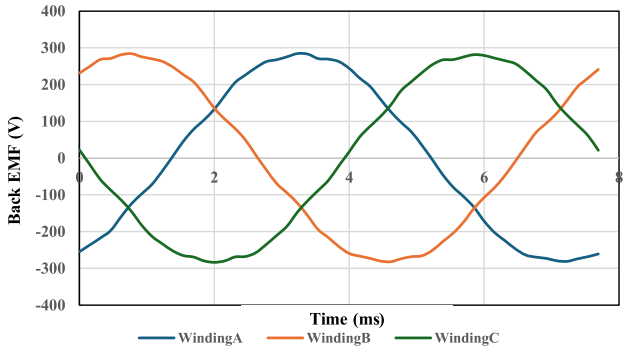

Fig. 5. Back EMF waveform at no load.

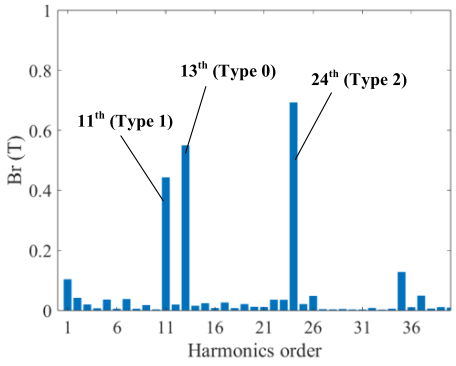

Fig. 6. FFT analysis of flux density distribution.

approximately 196 turns of coil per stator slot under a filling factor of 0.5, and given that this is a single-layer winding design, the maximum output of the back EMF can reach approximately 284 V.

To validate the selection of working harmonics, the Fourier analysis of the air-gap magnetic flux density was performed, as shown in Fig. 6. It can be observed that the 11th, 13th, and 24th harmonics are the primary working harmonics. The 13th harmonic corresponds to the unmodulated Type 0 harmonic, while the 11th and 24th harmonics represent the modulated Types 1 and 2 harmonics, respectively, further confirming the correctness of the underlying principles.

The torque performance of the machine is a critical parameter among the various aspects of its characteristics and serves as an important indicator for evaluating the suitability and

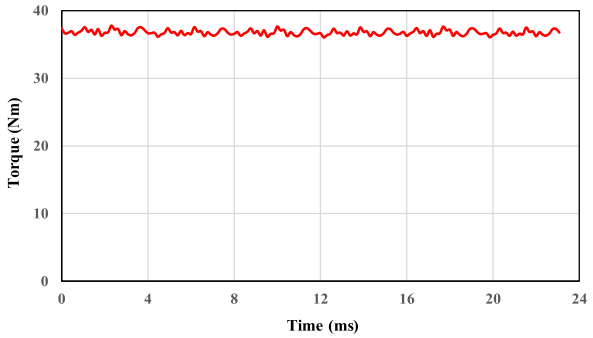

Fig. 7. Torque waveform at load after three cycles.

TABLE II

TORQUE PARAMETERS OF GENERATOR AND COMPARISON

Items	Unit	BFRPMG	PMSG
T_{max}	Nm	37.79	5-30
T_{avg}	Nm	36.8	1-10
T_density	Nm/L	26.25	2-10
T_ ripple	N/A	4.35%	5-20%

reliability. Fig. 7 illustrates the torque waveform of this design over three cycles. The comprehensive simulation analysis was conducted under the condition of a current density of 6 A/mm^2 and a speed of 600 r/min with a load applied. It can be observed that the machine can ensure a stable output.

The parameters related to the torque of this generator and comparison with regular PM synchronous generator (PMSG) at the same volume are presented in Table II. The maximum torque of the generator can reach 37.79 Nm, with an average torque of 36.8 Nm, which constitutes a substantial output for PM generators, especially when compared to the mainstream wind power PMSG currently available on the market. Moreover, the torque density is measured at 26.25 Nm/L, exceeding the industry benchmark of 20 Nm/L. In addition, the torque ripple is recorded at 4.35%, significantly lower than the 10% standard commonly accepted in the industry. This indicates a higher level of stability in the torque output than regular PMSG.

The introduction of the voltage regulation ratio (VRR) concept is intended to evaluate the magnetic flux control capability of the generator, which is related to the maximum and minimum values of the back EMF. It is defined as follows:

$$\mathrm{VRR} = \frac{E_{\max} - E_{\min}}{E_{\max}} \times 100\%. \tag{10}$$

Fig. 8 shows the relationship between back EMF amplitude and the initial phase angle by FEM analysis. It can be found that the back EMF amplitude varies with the electrical angle, and at 0°, the amplitude is the largest. With the rotation in different directions, the amplitude decreases accordingly. The output of the back EMF is the performance of magnetic properties, and the decrease of the amplitude of the back EMF is also the effect of flux weakening. According to Fig. 8, $E_{\max}$ for the single-turn coil is obtained as 1.45 V, while $E_{\min}$ is 0.11 V. Consequently, the VRR is calculated to be 93%. The VRR calculated by the analytical method is 93.2%, which is close to the FEM results, and the accuracy of the analysis is illustrated. The analytical method is related to the back EMF amplitude of harmonic Types 0, 1, and 2, which are E_0 and

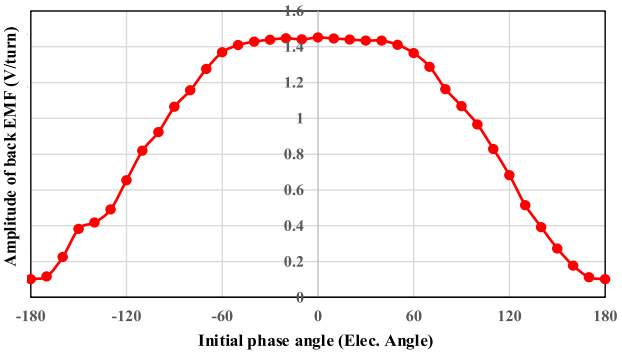

Fig. 8. Curves of back EMF amplitude versus the initial phase angle.

$E_{1,2}$, and $E_{\min} = |E_0 - E_{1,2}|$ and $E_{\max} = E_0 + E_{1,2}$. A higher VRR indicates a stronger magnetic flux control capability, which in turn signifies a more robust voltage control ability.

V. Conclusion

This article introduces the design of a radial PM generator. Based on the development of the bidirectional flux modulation effect derived from the principle of flux modulation, the adjustable modulation ring featuring embedded PMs has been designed. This design enhances the overall magnetic flux control capability and enables mechanical flux weakening, thereby improving the overall reliability of the system. The position of the adjustable modulation ring is controlled by a servo motor with almost zero speed, and the loss of the servo motor is usually less than 10 W, far less than the additional loss of the electric method of flux weakening; the overall efficiency of the generator is also improved.

The introduction to the VRR reflects the strong magnetic flux control capability, as well as its significant voltage regulation ability and range, which is reached to 93%. This further indicates that the design is suitable for VSCAV control in wind power generation, making it particularly applicable for regions that are remote from the electrical grid. In addition, the torque performance designed in this article demonstrates considerable utilization value for wind power generation. Both the torque density and average torque surpass those of the current mainstream generators available in the market. Furthermore, it exhibits minimal fluctuation, highlighting its stability in operational conditions.

By selecting the appropriate working harmonics, this design can achieve the output of back EMF using only a single set of windings and features a single-layer design. Compared to the dual-layer, dual-set windings used in most conventional machines, this design simplifies the manufacturing process and reduces production costs. In practical applications, it offers high reference value.

Acknowledgment

This work was supported by the National Natural Science Foundation of China under Project 52077187 and in part by Hong Kong Polytechnic University under Grant P0048560.

References

[1] G. S. Reddy and K. S. Rao, "Analysis on feasibility of electric power generation-via-wind power," in *Proc. IEEE 7th Power India Int. Conf. (PIICON)*, Bikaner, India, Nov. 2016, pp. 1–5.

[2] X. Zhou, Z. Wang, Y. Ma, and Z. Gao, "An overview on development of wind power generation," in *Proc. IEEE Int. Conf. Mechatronics Autom. (ICMA)*, Yinchuan, China, Aug. 2018, pp. 2042–2046, doi: 10.1109/ICMA.2018.8484401.

[3] K. T. Chau, "Permanent magnet brushless motor drives," in *Electric Vehicle Machines and Drives*. Wiley, 2015, pp. 69–107.

[4] J. Chen, C. V. Nayar, and L. Xu, "Design and finite-element analysis of an outer-rotor permanent-magnet generator for directly coupled wind turbines," *IEEE Trans. Magn.*, vol. 36, no. 5, pp. 3802–3809, Sep. 2000, doi: 10.1109/20.908378.

[5] X. Yang, D. Patterson, and J. Hudgins, "Permanent magnet generator design and control for large wind turbines," in *Proc. IEEE Power Electron. Mach. Wind Appl.*, Denver, CO, USA, Jul. 2012, pp. 1–5.

[6] W. L. Soong, D. A. Staton, and T. J. E. Miller, "Design of a new axially-laminated interior permanent magnet motor," *IEEE Trans. Ind. Appl.*, vol. 31, no. 2, pp. 358–367, Mar./Apr. 1995.

[7] T. M. Jahns, "Flux-weakening regime operation of an interior permanent-magnet synchronous motor drive," *IEEE Trans. Ind. Appl.*, vol. IA-23, no. 4, pp. 681–689, Jul. 1987.

[8] T. M. Jahns, G. B. Kliman, and T. W. Neumann, "Interior permanent-magnet synchronous motors for adjustable-speed drives," *IEEE Trans. Ind. Appl.*, vol. IA-22, no. 4, pp. 738–747, Jul. 1986, doi: 10.1109/TIA.1986.4504786.

[9] J. Jiang, X. Zhang, X. Zhao, and S. Niu, "A novel winding switching control strategy for AC/DC hybrid-excited wind power generator," *IEEE Trans. Magn.*, vol. 57, no. 6, pp. 1–4, Jun. 2021, doi: 10.1109/TMAG.2021.3074926.

[10] J. Jiang, S. Niu, X. Zhao, and W. N. Fu, "A novel winding switching control strategy of a consequent-pole ferrite-PM hybrid-excited machine for electric vehicle application," *IEEE Trans. Magn.*, vol. 58, no. 2, pp. 1–5, Feb. 2022.

[11] S. Hemmati and M. Barigh, "A new approach for field weakening in a surface mounted permanent magnet synchronous motor by winding switching," in *Proc. 27th Iranian Conf. Electr. Eng. (ICEE)*, Yazd, Iran, Apr. 2019, pp. 509–514.

[12] X. Zhao, J. Jiang, S. Niu, and Q. Wang, "Slot-PM-assisted hybrid reluctance generator with self-excited DC source for stand-alone wind power generation," *IEEE Trans. Magn.*, vol. 58, no. 2, pp. 1–6, Feb. 2022.

[13] Y. Wang, Z. Deng, and X. Wang, "A parallel hybrid excitation flux-switching generator DC power system based on direct torque linear control," *IEEE Trans. Energy Convers.*, vol. 27, no. 2, pp. 308–317, Jun. 2012, doi: 10.1109/TEC.2012.2185826.

[14] J. Jiang and S. Niu, "A novel slot PM-assisted hybrid magnet memory machine," *IEEE Trans. Magn.*, vol. 58, no. 8, pp. 1–6, Aug. 2022, doi: 10.1109/TMAG.2022.3142192.

[15] H. Yang, H. Lin, Z. Q. Zhu, S. Niu, S. Lyu, and H. Zheng, "A novel stator spoke-type hybrid magnet memory machine," in *Proc. IEEE Int. Electric Mach. Drives Conf. (IEMDC)*, San Diego, CA, USA, May 2019, pp. 1576–1580, doi: 10.1109/IEMDC.2019.8785325.

[16] Z. Q. Zhu, M. M. J. Al-Ani, X. Liu, and B. Lee, "A mechanical flux weakening method for switched flux permanent magnet machines," *IEEE Trans. Energy Convers.*, vol. 30, no. 2, pp. 806–815, Jun. 2015, doi: 10.1109/TEC.2014.2380851.

[17] G. Zhou, T. Miyazaki, S. Kawamata, D. Kaneko, and N. Hino, "Development of variable magnetic flux motor suitable for electric vehicle," in *Proc. Int. Power Electron. Conf.*, Sapporo, Japan, Jun. 2010, pp. 2171–2174.

[18] M. Jiang and S. Niu, "Novel mechanical flux-weakening design of a spoke-type permanent magnet generator for stand-alone power supply," *Appl. Sci.*, vol. 13, no. 4, p. 2689, Feb. 2023.

[19] M. Jiang and S. Niu, "A high-order harmonic compound rotor based brushless dual-electrical-port dual-mechanical-port machine," *IEEE Trans. Ind. Electron.*, vol. 71, no. 6, pp. 5463–5473, Jun. 2024.

[20] M. Jiang, S. Niu, and W. Wu, "Design and analysis of a novel dual-rotor transverse flux permanent magnet machine," in *Proc. 49th Annu. Conf. IEEE Ind. Electron. Soc.*, Singapore, Oct. 2023, pp. 1–6.

[21] Y. Wang, S. Niu, and W. Fu, "A novel dual-rotor bidirectional flux-modulation PM generator for stand-alone DC power supply," *IEEE Trans. Ind. Electron.*, vol. 66, no. 1, pp. 818–828, Jan. 2019.

[22] Q. Wang, S. Niu, and L. Yang, "Design optimization of a novel scale-down hybrid-excited dual permanent magnet generator for direct-drive wind power application," *IEEE Trans. Magn.*, vol. 54, no. 3, pp. 1–4, Mar. 2018.